

On Constraints Between $\Delta\alpha_{\text{had}}(M_Z^2)$ and $(g_\mu - 2)_{\text{HVP}}$

Eduardo de Rafael

Aix-Marseille Univ, Université de Toulon, CNRS, CPT, Marseille, France

Abstract

I discuss the possibility of estimating the shift $\delta\Delta\alpha(M_Z^2)$ on the running of the EM-coupling to the M_Z scale, induced by the discrepancy Δa_μ between two precise determinations of the hadronic vacuum polarization contribution to $g_\mu - 2$. It is shown that the size of Δa_μ implies rigorous bounds on the $\delta\Delta\alpha(M_Z^2)$ -shift. Any extra contribution to this minimal shift necessarily depends on the specific shape of the underlying spectral function $\frac{1}{\pi}\text{Im}\Delta(t)$ responsible for the Δa_μ -discrepancy. I show that, in the case of a quark model, the total $\Delta\alpha(M_Z^2)$ -shift remains small. I also discuss the scenario where $\frac{1}{\pi}\text{Im}\Delta(t)$ is a constant in a finite t -region and show that in this case, up to a $t_{\text{max}} \lesssim 5 \text{ GeV}^2$, the size of the total $\delta\Delta\alpha_{\text{had}}^{(5)}(M_Z^2)$ -shift, remains below or of the order of the present error value on $\Delta\alpha_{\text{had}}^{(5)}(M_Z^2)$.

I Introduction.

Testing the EW-Standard Model requires knowledge of the running of the EM-coupling induced by the hadronic interactions, from the low-energy measured value $\alpha = 1/137.036\dots$ up to the scale of the M_Z -mass: $M_Z = 91.1876 \pm 0.0021$ GeV. This running is encoded in a quantity called $\Delta\alpha_{\text{had}}(M_Z^2)$, which in terms of the hadronic spectral function $\frac{1}{\pi}\text{Im}\Pi_{\text{had}}(t)$ is given by the principal value integral:

$$\Delta\alpha_{\text{had}}(M_Z^2) = \text{PV} \int_{t_0=4m_\pi^2}^{\infty} \frac{dt}{t} \frac{M_Z^2}{M_Z^2 - t} \frac{1}{\pi} \text{Im}\Pi_{\text{had}}(t), \quad (1.1)$$

and contributes to the running of α at the M_Z -scale via the relation:

$$\alpha(M_Z^2) = \frac{\alpha}{1 - \Delta\alpha_{\text{had}}(M_Z^2) - \Delta\alpha_{\text{lep}}(M_Z^2)}, \quad (1.2)$$

where

$$\Delta\alpha_{\text{lep}}(M_Z^2) = (314.979 \pm 0.002) \times 10^{-4} \quad (1.3)$$

is the contribution due to the EM-couplings of the leptons [1, 2].

The same hadronic spectral function governs the hadronic vacuum polarization (HVP) contribution to the muon anomalous magnetic moment via the equivalent integral representations [3, 4, 5, 6]:

$$a_\mu^{\text{HVP}} = \frac{\alpha}{\pi} \int_{t_0}^{\infty} \frac{dt}{t} \int_0^1 dx \underbrace{\frac{x^2(1-x)}{x^2 + \frac{t}{m_\mu^2}(1-x)}}_{K(t)} \frac{1}{\pi} \text{Im}\Pi_{\text{had}}(t), \quad (1.4)$$

$$= -\frac{\alpha}{\pi} \int_0^1 dx (1-x) \Pi_{\text{had}}\left(\frac{x^2}{1-x} m_\mu^2\right), \quad (1.5)$$

where

$$-\Pi_{\text{had}}(Q^2) = \int_{t_0}^{\infty} \frac{dt}{t} \frac{Q^2}{Q^2 + t} \frac{1}{\pi} \text{Im}\Pi_{\text{had}}(t), \quad Q^2 \equiv \frac{x^2}{1-x} m_\mu^2. \quad (1.6)$$

is the hadronic self-energy in the Euclidean and the optical theorem relates the spectral function $\frac{1}{\pi}\text{Im}\Pi_{\text{had}}(t)$ to the observable one-photon annihilation cross-section:

$$\sigma(t)_{e^+e^- \rightarrow \text{had}} \underset{m_e \rightarrow 0}{\sim} \frac{4\pi^2\alpha}{t} \frac{1}{\pi} \text{Im}\Pi_{\text{had}}(t). \quad (1.7)$$

This is the way that experimental data-driven determinations of $\Delta\alpha_{\text{had}}(M_Z^2)$ and a_μ^{HVP} have been obtained (see refs. [8, 9] and the recent review in ref. [10]).

In ref. [9], the contribution to $\Delta\alpha_{\text{had}}(M_Z^2)$ from the hadronic flavours induced by u, d, s, c, b quarks called $\Delta\alpha_{\text{had}}^{(5)}(M_Z^2)$, has been obtained¹ using experimental data up to

$$\sqrt{t_{\text{max}}} = 11.199 \text{ GeV}, \quad (1.8)$$

and pQCD beyond that energy with the overall result

$$\Delta\alpha_{\text{had}}^{(5)}(M_Z^2) = (276.09 \pm 1.12) \times 10^{-4}. \quad (1.9)$$

On the other hand, there is a recent LQCD determination of a_μ^{HVP} reported by the BMWc collaboration [11], which differs significantly from the data-driven results on $\sigma(t)_{e^+e^- \rightarrow \text{had}}$ quoted in refs. [8, 9]. To be precise, let me compare the lowest order HVP result of ref. [9] (which has the largest discrepancy) with the one in ref. [11] i.e.,

$$a_\mu^{\text{HVP}}(\text{KNT}) = (692.78 \pm 2.42) \times 10^{-10}, \quad \text{versus} \quad a_\mu^{\text{HVP}}(\text{BMWc}) = (708.7 \pm 5.3) \times 10^{-10}. \quad (1.10)$$

¹For other determinations of $\Delta\alpha_{\text{had}}(M_Z^2)$, all compatible within errors, see e.g. Table 6 in this reference and ref. [10].

This discrepancy

$$\Delta a_\mu \equiv a_\mu^{\text{HVP}}(\text{BMWc}) - a_\mu^{\text{HVP}}(\text{KNT}) = (15.92 \pm 5.83) \times 10^{-10} \quad (1.11)$$

of 2.7σ , has prompted a reexamination of the question raised sometime ago [12]:

At what precision is $\Delta\alpha_{\text{had}}^{(5)}(M_Z^2)$ constrained by an accurate determination of a_μ^{HVP} ?

Possible scenarios have been discussed in refs. [13, 14] that, though model dependent, suggest potential inconsistencies between the $a_\mu^{\text{HVP}}(\text{BMWc})$ result and the present value for $\Delta\alpha_{\text{had}}^{(5)}(M_Z^2)$ in Eq. (1.9) ².

The purpose of this note is to address the question above from a new perspective. In the next section, I discuss a model-independent analysis of the observables a_μ^{HVP} and $\Delta\alpha_{\text{had}}^{(5)}(M_Z^2)$ within the Mellin-Barnes Representation framework. Section III discusses properties of the *first moment* related to these two observables. Rigorous bounds on the size of the shift implied on $\Delta\alpha_{\text{had}}^{(5)}(M_Z^2)$ by the Δa_μ -discrepancy, *when only the value of Δa_μ is known*, are then derived in Section IV. Alternative phenomenological models to those discussed in ref. [13] are then presented in Section V with conclusions in Section VI.

II Mellin-Barnes Representations.

Mellin-Barnes representations are particularly useful to obtain asymptotic expansions of functions. In the case of a_μ^{HVP} [16]:

$$a_\mu^{\text{HVP}} = \left(\frac{\alpha}{\pi}\right) \frac{m_\mu^2}{t_0} \frac{1}{2\pi i} \int_{c_s - i\infty}^{c_s + i\infty} ds \left(\frac{m_\mu^2}{t_0}\right)^{-s} \mathcal{F}(s) \mathcal{M}(s), \quad c_s \equiv \text{Re}(s) \in]0, 1[, \quad (2.1)$$

where $\mathcal{F}(s) = -\Gamma(3 - 2s) \Gamma(-3 + s) \Gamma(1 + s)$, and

$$\mathcal{M}(s) = \int_{t_0}^{\infty} \frac{dt}{t} \left(\frac{t}{t_0}\right)^{s-1} \frac{1}{\pi} \text{Im}\Pi_{\text{had}}(t), \quad (2.2)$$

is the Mellin transform of the spectral function. This representation has been proposed as a possible way to obtain successive approximations to a_μ^{HVP} from the knowledge of the moments $\mathcal{M}(s)$ at $s = 0, -1, -2 \dots$ and their extrapolation at all s -values using Mellin-Barnes approximants (see refs. [17, 18] and references therein).

There is also a similar representation for $\Delta\alpha_{\text{had}}(M_Z^2)$:

$$\Delta\alpha_{\text{had}}(M_Z^2) = \frac{1}{2\pi i} \int_{c_s - i\infty}^{c_s + i\infty} ds \int_{t_0}^{\infty} \frac{dt}{t} \frac{1}{\pi} \text{Im}\Pi_{\text{had}}(t) \left(\frac{t}{M_Z^2}\right)^{-s} \Gamma(s) \Gamma(1 - s) \frac{\pi}{\Gamma(\frac{1}{2} + s) \Gamma(\frac{1}{2} - s)}, \quad (2.3)$$

which differs by the factor $\frac{\pi}{\Gamma(\frac{1}{2} + s) \Gamma(\frac{1}{2} - s)}$ [19], when compared to the representation in the Euclidean:

$$\Delta\alpha_{\text{had}}(-M_Z^2) = \frac{1}{2\pi i} \int_{c_s - i\infty}^{c_s + i\infty} ds \int_{t_0}^{\infty} \frac{dt}{t} \frac{1}{\pi} \text{Im}\Pi_{\text{had}}(t) \left(\frac{t}{M_Z^2}\right)^{-s} \Gamma(s) \Gamma(1 - s). \quad (2.4)$$

Restricting the integration over the spectral function to an upper scale t_{max} , as we shall later do, one has

$$\Delta\alpha_{\text{had}}^{(5)}(M_Z^2)_{\text{data}} = \frac{1}{2\pi i} \int_{c_s - i\infty}^{c_s + i\infty} ds \left(\frac{t_{\text{max}}}{M_Z^2}\right)^{-s} \tilde{\mathcal{M}}(s) \frac{\Gamma(s) \Gamma(1 - s)}{\Gamma(\frac{1}{2} + s) \Gamma(\frac{1}{2} - s)} \pi, \quad (2.5)$$

² See also ref. [15] which has appeared after the completion of this work.

where $\tilde{\mathcal{M}}(s)$ is now the restricted Mellin transform

$$\tilde{\mathcal{M}}(s) = \int_{t_0}^{t_{\max}} \frac{dt}{t} \left(\frac{t}{t_{\max}} \right)^{-s} \frac{1}{\pi} \text{Im}\Pi_{\text{had}}(t). \quad (2.6)$$

This representation governs the asymptotic expansion of $\Delta\alpha_{\text{had}}^{(5)}(M_Z^2)_{\text{data}}$ in terms of the ratio $\left(\frac{t_{\max}}{M_Z^2}\right)$. The series expansion in this ratio is fixed by the successive singularities at the left of the fundamental strip: $0 < \text{Re } c_s < 1$, i.e. at $s = 0, -1, -2, \dots$ of the integrand in the r.h.s. of Eq. (2.5), and the coefficients are proportional to the moments:

$$\int_{t_0}^{t_{\max}} \frac{dt}{t} \left(\frac{t}{t_{\max}} \right)^n \frac{1}{\pi} \text{Im}\Pi_{\text{had}}(t), \quad n = 0, 1, 2, \dots, \quad (2.7)$$

which give information about the spectral function $\frac{1}{\pi} \text{Im}\Pi_{\text{had}}(t)$ in a different region to the one provided by the moments:

$$\int_{t_0}^{\infty} \frac{dt}{t} \left(\frac{t_0}{t} \right)^n \frac{1}{\pi} \text{Im}\Pi_{\text{had}}(t), \quad n = 1, 2, \dots, \quad (2.8)$$

which govern the $(g_\mu - 2)_{\text{had}}$ contribution [16, 17, 18]. Therefore, within this perspective, the possibility of relating the two observables $\Delta\alpha_{\text{had}}^{(5)}(M_Z^2)$ and $(g_\mu - 2)_{\text{had}}$ seems *a priori* a rather difficult task, unless of course one uses data or a model for the hadronic spectral function, or performs fully dedicated LQCD evaluations of both observables.

Moments like those in Eq. (2.7) can be related to the contour integrals (where Q^2 is now a complex variable) [20]:

$$\frac{1}{2\pi i} \oint_{|Q^2|=t_{\max}} \frac{dQ^2}{Q^2} \left(\frac{Q^2}{t_{\max}} \right)^n \Pi_{\text{had}}(Q^2) = (-1)^{n+1} \int_{t_0}^{t_{\max}} \frac{dt}{t} \left(\frac{t}{t_{\max}} \right)^n \frac{1}{\pi} \text{Im}\Pi_{\text{had}}(t), \quad (2.9)$$

which define a particular case of Finite Energy Sum Rules. The experimental determination of the integrals on the r.h.s. can thus be confronted, for sufficiently large t_{\max} -values, to a theoretical calculation of the l.h.s. using pQCD and the OPE at large- Q^2 values.

By contrast, the moments in Eq. (2.8) are related to derivatives of the self-energy function $\Pi_{\text{had}}(Q^2)$ at $Q^2 = 0$ [16]:

$$\frac{(-1)^{n+1}}{(n+1)!} (t_0)^{n+1} \underbrace{\left(\frac{\partial^{n+1}}{(\partial Q^2)^{n+1}} \Pi(Q^2) \right)_{Q^2=0}}_{\text{LQCD}} = \underbrace{\int_{t_0}^{\infty} \frac{dt}{t} \left(\frac{t_0}{t} \right)^{1+n} \frac{1}{\pi} \text{Im}\Pi(t)}_{\text{Experiment}}, \quad n = 0, 1, 2, \dots \quad (2.10)$$

As discussed in refs. [16, 17, 18] they provide excellent tests to confront LQCD evaluations of the l.h.s. with experimental results, but they invoke a totally different Q^2 -region to the one which applies to Eq. (2.9).

III The First Moment.

I want to focus attention on the first moment $n = 0$ in Eq. (2.10):

$$-t_0 \frac{\partial \Pi_{\text{had}}(Q^2)}{\partial Q^2} \Big|_{Q^2=0} = \int_{t_0}^{\infty} \frac{dt}{t} \frac{t_0}{t} \frac{1}{\pi} \text{Im}\Pi_{\text{had}}(t). \quad (3.1)$$

A long time ago, the authors of ref. [21] showed that there is an upper and lower bound for a_μ^{HVP} in terms of this moment, namely:

$$\frac{\alpha}{\pi} \frac{1}{3} \frac{m_\mu^2}{t_0} \left(\int_{t_0}^{\infty} \frac{dt}{t} \frac{t_0}{t} \frac{1}{\pi} \text{Im}\Pi_{\text{had}}(t) \right) \left[1 - f \left(\frac{t_0}{m_\mu^2} \right) \right] < a_\mu^{\text{HVP}} < \frac{\alpha}{\pi} \frac{1}{3} \frac{m_\mu^2}{t_0} \left(\int_{t_0}^{\infty} \frac{dt}{t} \frac{t_0}{t} \frac{1}{\pi} \text{Im}\Pi_{\text{had}}(t) \right), \quad (3.2)$$

where

$$f\left(\frac{t_0}{m_\mu^2}\right) = 3 \int_0^1 dx \frac{x^4}{x^2 + \frac{t_0}{m_\mu^2}(1-x)} = 0.36655, \quad \text{for } t_0 = 4m_\pi^2. \quad (3.3)$$

The bounds follow from the observation that the kernel $K(t)$ in Eq. (1.4) can be written as follows:

$$K(t) = \frac{m_\mu^2}{t} \int_0^1 dx \left[x^2 - \underbrace{\left(\frac{x^4}{x^2 + \frac{t}{m_\mu^2}(1-x)} \right)}_{\frac{1}{3}f\left(\frac{t}{m_\mu^2}\right)} \right], \quad (3.4)$$

and the fact that, within the t -integration range $t_0 < t < \infty$,

$$0 < f\left(\frac{t}{m_\mu^2}\right) < f\left(\frac{t_0}{m_\mu^2}\right). \quad (3.5)$$

In the language of the Mellin-Barnes representation of Section II, the upper bound in Eq. (3.2) corresponds to retaining only the leading term in the singular expansion of $\mathcal{F}(s)$, i.e. the contribution from the simple pole at $s = 0$. This contribution can be seen as induced by an effective local operator $\partial^\lambda F^{\mu\nu} \partial_\lambda F_{\mu\nu}$ to which I shall later come back. The other terms of the singular expansion of $\mathcal{F}(s)$ give successive corrections to the upper-bound. The simple poles generate the moments in Eq. (2.10) for $n \geq 1$, which can also be seen as induced by local operators of higher and higher dimension. The double poles generate the log-weighted moments discussed in ref. [16]:

$$\int_{t_0}^\infty \frac{dt}{t} \left(\frac{t_0}{t}\right)^n \log \frac{t}{t_0} \frac{1}{\pi} \text{Im}\Pi_{\text{had}}(t), \quad n = 1, 2, \dots, \quad (3.6)$$

and can be seen as generated by successive non-local operators. The lower bound in Eq. (3.2) is a rigorous bound to the contribution from the sum of all the terms of the singular expansion of $\mathcal{F}(s)$ beyond the leading one and, therefore, to the total effect of the underlying string of local and non-local operators which give rise to these terms. The remarkable feature about the simplicity of the resulting lower bound in Eq (3.2) is that *it is proportional to the same leading moment which fixes the upper bound!* Therefore, this lower bound can also be seen as induced by an effective local operator of the type $\partial^\lambda F^{\mu\nu} \partial_\lambda F_{\mu\nu}$ modulated, however, by a different coupling.

In the case of the electron $(g_e - 2)_{\text{HVP}}$ the bounds in Eq (3.2) are impressive. Using the experimental determination of the lowest HVP-moment ³:

$$\int_{t_0}^\infty \frac{dt}{t} \frac{t_0}{t} \frac{1}{\pi} \text{Im}\Pi_{\text{had}}(t) = (0.7176 \pm 0.0026) \times 10^{-3}, \quad (3.7)$$

one finds:

$$1.8550 \times 10^{-12} < a_e^{\text{HVP}} < 1.8687 \times 10^{-12}, \quad (3.8)$$

which corresponds to an accuracy of 0.37%. I recall that the lowest order HVP experimental determination in the case of the electron anomaly gives [9]:

$$a_e^{\text{HVP}} = 1.8608(66) \times 10^{-12}. \quad (3.9)$$

The contribution from the HVP-moment in Eq. (3.7) to $\Delta\alpha_{\text{had}}^{(5)}(M_Z^2)$ in Eq. (1.1) is a small fraction of the total:

$$\Delta\alpha_{\text{had}}^{(5)}(M_Z^2) = \underbrace{\int_{t_0}^\infty \frac{dt}{t} \frac{t_0}{t} \frac{1}{\pi} \text{Im}\Pi_{\text{had}}(t)}_{7.176 \times 10^{-4}} + \text{PV} \int_{t_0}^\infty \frac{dt}{t} \left(\frac{M_Z^2}{M_Z^2 - t} - \frac{t_0}{t} \right) \frac{1}{\pi} \text{Im}\Pi_{\text{had}}(t), \quad (3.10)$$

but, as we shall see next, it gives the key to relate the two observables $\Delta\alpha_{\text{had}}^{(5)}(M_Z^2)$ and $(g_\mu - 2)_{\text{HVP}}$.

³Private communication from the authors of ref. [9].

IV The Effective Operator $\partial^\lambda F^{\mu\nu} \partial_\lambda F_{\mu\nu}$ and Rigorous Bounds.

The effective operator which governs the size of the slope at the origin of the photon self-energy, and therefore the first moment of the underlying spectral function, is the dimension $d = 6$ operator

$$\frac{1}{\Lambda^2} \partial^\lambda F^{\mu\nu} \partial_\lambda F_{\mu\nu}. \quad (4.1)$$

For the HVP-contribution in particular we have

$$-\left. \frac{\partial \Pi_{\text{had}}(Q^2)}{\partial Q^2} \right|_{Q^2=0} = \frac{\alpha}{\pi} \frac{1}{\Lambda_{\text{had}}^2}, \quad (4.2)$$

and from Eq. (2.10)

$$\frac{\alpha}{\pi} \frac{t_0}{\Lambda_{\text{had}}^2} = \int_{t_0}^{\infty} \frac{dt}{t} \frac{t_0}{t} \frac{1}{\pi} \text{Im} \Pi_{\text{had}}(t). \quad (4.3)$$

The experimental value of the scale Λ_{had} which follows from Eq. (3.7) is

$$\Lambda_{\text{had}} = (0.502 \pm 0.001) \text{ GeV}, \quad (4.4)$$

which, as expected, is a scale of the order of the ρ -mass.

The Δa_μ discrepancy in Eq. (1.11) can be interpreted as an excess, in some (so far) unknown t -range, of the underlying spectral function which results in the BMWc-evaluation, as compared to the spectral function which has been used in the KNT-evaluation i.e.,

$$\Delta a_\mu = \frac{\alpha}{\pi} \int_{t_0}^{\infty} \frac{dt}{t} K(t) \frac{1}{\pi} \text{Im} \Delta(t), \quad (4.5)$$

where

$$\frac{1}{\pi} \text{Im} \Delta(t) \equiv \frac{1}{\pi} \text{Im} \Pi_{\text{BMWc}}(t) - \frac{1}{\pi} \text{Im} \Pi_{\text{KNT}}(t) \geq 0 \quad \text{for } t_0 \leq t \leq \infty. \quad (4.6)$$

This difference of spectral functions can be seen as generated, at least in part, by an effective local operator of the type in Eq. (4.1) which induces an effective moment

$$\frac{\alpha}{\pi} \frac{t_0}{\Lambda_{\text{eff}}^2} = \int_{t_0}^{\infty} \frac{dt}{t} \frac{t_0}{t} \frac{1}{\pi} \text{Im} \Delta(t), \quad (4.7)$$

and in terms of which, the bounds in Eq. (3.2) when applied to Δa_μ , give

$$\frac{\alpha}{\pi} \frac{1}{3} \frac{m_\mu^2}{t_0} \left[1 - f\left(\frac{t_0}{m_\mu^2}\right) \right] \left(\frac{\alpha}{\pi} \frac{t_0}{\Lambda_{\text{eff}}^2} \right) < \Delta a_\mu < \frac{\alpha}{\pi} \frac{1}{3} \frac{m_\mu^2}{t_0} \left(\frac{\alpha}{\pi} \frac{t_0}{\Lambda_{\text{eff}}^2} \right). \quad (4.8)$$

Including the error of Δa_μ in Eq. (1.11) so as to take the largest and smallest values of the discrepancy, fixes the extreme values of the scale Λ_{eff}^2 to be within the limits:

$$\Lambda_{\text{eff}}^2 = 19.89 \text{ GeV}^2 \text{ (from the upper bound)} \quad \text{and} \quad \Lambda_{\text{eff}}^2 = 5.85 \text{ GeV}^2 \text{ (from the lower bound)}. \quad (4.9)$$

These two scales fix the range of couplings of the effective operator which is at the origin, at least in part, of the anomaly discrepancy. Their effect on $\Delta \alpha_{\text{had}}^{(5)}(M_Z^2)$ is to add a shift to the underlined term in the r.h.s. of Eq. (3.10):

$$\begin{aligned} \Delta \alpha_{\text{had}}^{(5)}(M_Z^2) &\Rightarrow \underbrace{\int_{t_0}^{\infty} \frac{dt}{t} \frac{t_0}{t} \frac{1}{\pi} \text{Im} \Pi_{\text{had}}(t)} + \frac{\alpha}{\pi} \frac{t_0}{\Lambda_{\text{eff}}^2} + \text{PV} \int_{t_0}^{\infty} \frac{dt}{t} \left(\frac{M_Z^2}{M_Z^2 - t} - \frac{t_0}{t} \right) \frac{1}{\pi} \text{Im} \Pi_{\text{had}}(t) \quad (4.10) \\ &= \underbrace{\frac{\alpha}{\pi} \frac{t_0}{\Lambda_{\text{eff}}^2}}_{\text{shift}} + \text{PV} \int_{t_0}^{\infty} \frac{dt}{t} \frac{M_Z^2}{M_Z^2 - t} \frac{1}{\pi} \text{Im} \Pi_{\text{had}}(t), \quad (4.11) \end{aligned}$$

with the shift constrained by the upper and lower bounds in Eq. (4.9) to be within the limits:

$$\frac{\alpha}{\pi} \underbrace{\frac{t_0}{19.89 \text{ GeV}^2}}_{0.091 \times 10^{-4}} \leq \frac{\alpha}{\pi} \frac{t_0}{\Lambda_{\text{eff}}^2} \leq \frac{\alpha}{\pi} \underbrace{\frac{t_0}{5.85 \text{ GeV}^2}}_{0.309 \times 10^{-4}}. \quad (4.12)$$

We find, therefore, that the accepted range of the minimal shift on $\Delta\alpha_{\text{had}}^{(5)}(M_Z^2)$ induced by the effective moment in Eq. (4.7) is rather small. In fact, the higher value is about four times smaller than the error 1.12×10^{-4} in the result in Eq. (1.9). In the absence of any information about the shape of the spectral function $\frac{1}{\pi}\text{Im}\Delta(t)$, this is as much as may be rigorously said about the size of the shift implied on $\Delta\alpha_{\text{had}}^{(5)}(M_Z^2)$.

Notice that as the discrepancy Δa_μ becomes smaller and smaller, Eq.(4.8) shows that Λ_{eff}^2 becomes larger and larger and, hence, the shift in Eq.(4.11) (the first term) smaller and smaller. By contrast, as the discrepancy Δa_μ becomes larger and larger Λ_{eff}^2 becomes smaller and smaller and, hence, the shift in Eq.(4.11) larger and larger.

Any extra contribution to the minimal shift in Eq. (4.12) is encoded in the difference

$$\text{PV} \int_{t_0}^{\infty} \frac{dt}{t} \frac{M_Z^2}{M_Z^2 - t} \frac{1}{\pi} \text{Im}\Delta(t) - \frac{\alpha}{\pi} \frac{t_0}{\Lambda_{\text{eff}}^2}, \quad (4.13)$$

with $\text{Im}\Delta(t)$ defined in Eq. (4.6), and its size depends on the specific shape of the underlying BMWc-spectral function.

V Phenomenological Models.

V.1 The Constituent Chiral Quark Model

Models of $\frac{1}{\pi}\text{Im}\Delta(t)$ which lead to much larger shifts to $\Delta\alpha_{\text{had}}^{(5)}(M_Z^2)$ than the minimal bounds in Eq. (4.12) have been disused in refs. [13, 14]. However, it is also possible to construct models that don't give such large shifts. The simple constituent chiral quark model (C χ QM) ⁴ may be used to illustrate this. The hadronic spectral function in this model:

$$\frac{1}{\pi} \text{Im}\Pi_{\chi\text{QM}}(t, M) = \frac{\alpha}{\pi} \frac{5}{3} N c \frac{1}{3} \left(1 + \frac{2M^2}{t}\right) \sqrt{1 - \frac{4M^2}{t}} \theta(t - 4M^2), \quad (5.1)$$

only depends on a M -mass parameter which can be adjusted so as to reproduce the central values of either the $a_\mu^{\text{HVP}}(\text{BMWc})$ or the $a_\mu^{\text{HVP}}(\text{KNT})$ determinations. These choices result in the values:

$$M_{\text{BMWc}} = 0.292 \text{ GeV} \quad \text{and} \quad M_{\text{KNT}} = 0.296 \text{ GeV}, \quad (5.2)$$

and the relevant spectral function is then

$$\frac{1}{\pi} \text{Im}\Delta_{\text{model}}(t) = \frac{1}{\pi} \text{Im}\Pi_{\chi\text{QM}}(t, M_{\text{BMWc}}) - \frac{1}{\pi} \text{Im}\Pi_{\chi\text{QM}}(t, M_{\text{KNT}}), \quad (5.3)$$

which has a shape as shown (in 10^{-3} -units) in Fig. 1 (the cusp in the figure corresponds to the threshold opening at $4M_{\text{KNT}}^2 = 0.350 \text{ GeV}^2$). The shift induced on $\Delta\alpha_{\text{had}}^{(5)}(M_Z^2)$ is then given by the integral

$$\text{PV} \int_{t_0=4m_\pi^2}^{\infty} \frac{dt}{t} \frac{M_Z^2}{M_Z^2 - t} \frac{1}{\pi} \text{Im}\Delta_{\text{model}}(t) = 0.42 \times 10^{-4}, \quad (5.4)$$

which, as expected, results in a number somewhat larger than the upper bound in Eq. (4.12).

⁴ see ref. [22] for details

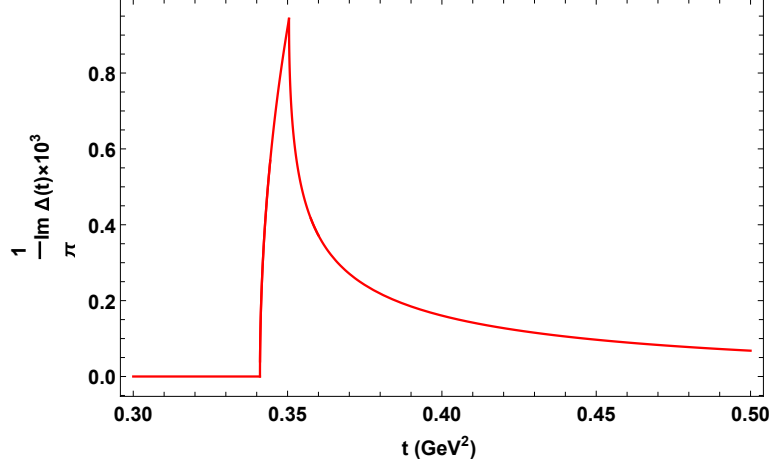


Figure 1:

Shape of the difference of spectral functions in Eq. (5.3) plotted in 10^{-3} units.

V.2 Beyond the Minimal Bounds

It would be nice to have some guidance to go beyond the minimal rigorous bounds previously discussed. In that respect I propose the following approach: it seems reasonable to assume that the region where the underlying spectral functions are responsible for the Δa_μ discrepancy is a finite region in the t -integration range i.e.,

$$\Delta a_\mu \equiv \frac{\alpha}{\pi} \int_{t_{\min}}^{t_{\max}} \frac{dt}{t} K(t) \frac{1}{\pi} \text{Im} \Delta(t), \quad \text{with } t_{\min} \geq t_0; \quad (5.5)$$

and $t_{\max} \ll M_Z^2$ because in any case both evaluations of the anomaly are using pQCD beyond a certain energy. The total shift on $\Delta \alpha_{\text{had}}^{(5)}(M_Z^2)$ induced by the same spectral function is then given by the integral

$$\delta \Delta \alpha_{\text{had}}^{(5)}(M_Z^2) = \int_{t_{\min}}^{t_{\max}} \frac{dt}{t} \frac{M_Z^2}{M_Z^2 - t} \frac{1}{\pi} \text{Im} \Delta(t), \quad (5.6)$$

which is no longer a principal value integral. There is a Mellin-Barnes representation for this shift, similar to the one given in Eq. (2.5):

$$\delta \Delta \alpha_{\text{had}}^{(5)}(M_Z^2) = \frac{1}{2\pi i} \int_{c_s - i\infty}^{c_s + i\infty} ds \left(\frac{t_{\max}}{M_Z^2} \right)^{-s} \tilde{\mathcal{M}}(s) \frac{\Gamma(s) \Gamma(1-s)}{\Gamma(\frac{1}{2} + s) \Gamma(\frac{1}{2} - s)} \pi, \quad (5.7)$$

where $\tilde{\mathcal{M}}(s)$ is now the restricted Mellin transform of $\frac{1}{\pi} \text{Im} \Delta(t)$,

$$\tilde{\mathcal{M}}(s) = \int_{t_{\min}}^{t_{\max}} \frac{dt}{t} \left(\frac{t}{t_{\max}} \right)^{-s} \frac{1}{\pi} \text{Im} \Delta(t). \quad (5.8)$$

The leading contribution in the expansion which follows from Eq. (5.7) is precisely the one induced by the singularity of the integrand at $s = 0$ and, therefore,

$$\delta \Delta \alpha_{\text{had}}^{(5)}(M_Z^2) = \tilde{\mathcal{M}}(0) + \mathcal{O} \left(\frac{t_{\max}}{M_Z^2} \right), \quad (5.9)$$

with $\tilde{\mathcal{M}}(0)$ dominating largely the full contribution.

Let me now assume that $\frac{1}{\pi}\text{Im}\Delta(t)$ is a constant in the region $t_{\min} \leq t \leq t_{\max}$:

$$\frac{1}{\pi}\text{Im}\Delta(t) \equiv \beta \theta(t - t_{\min}) \theta(t_{\max} - t), \quad (5.10)$$

something which could well be the case if e.g. the Δa_μ discrepancy was due to a shift in a t -region of the spectrum that corresponds to an offset in its height. In this case

$$\Delta a_\mu = \beta \frac{\alpha}{\pi} \int_{t_{\min}}^{t_{\max}} \frac{dt}{t} K(t) \quad \text{and} \quad \tilde{\mathcal{M}}(0) = \beta \log \frac{t_{\max}}{t_{\min}}, \quad (5.11)$$

which neglecting $\mathcal{O}\left(\frac{t_{\max}}{M_Z^2}\right)$ terms in Eq. (5.9), results in a simple expression for the total $\delta\Delta\alpha_{\text{had}}^{(5)}(M_Z^2)$ -shift:

$$\delta\Delta\alpha_{\text{had}}^{(5)}(M_Z^2) = \frac{\Delta a_\mu}{\frac{\alpha}{\pi} \int_{t_{\min}}^{t_{\max}} \frac{dt}{t} K(t)} \log \frac{t_{\max}}{t_{\min}}. \quad (5.12)$$

As a numerical illustration of this result, I show in Fig. 2 the size of the $\delta\Delta\alpha_{\text{had}}^{(5)}(M_Z^2)$ -shift as a function of t_{\max} in the range $9m_\pi^2 \leq t_{\max} \leq 16 \text{ GeV}^2$ with $t_{\min} = 4m_\pi^2$. The thick red curve in the figure shows the $\delta\Delta\alpha_{\text{had}}^{(5)}(M_Z^2)$ -shift corresponding to the central value of the discrepancy Δa_μ in Eq. (1.11); the dashed curves the results of the same shift when including the upper and lower errors on Δa_μ . The thick green line shows the present experimental error of ± 1.12 on $\Delta\alpha_{\text{had}}^{(5)}(M_Z^2)$ in Eq. (1.9) in 10^{-4} units. The plot in this figure shows that up to a $t_{\max} \lesssim 5 \text{ GeV}^2$, the size of the $\delta\Delta\alpha_{\text{had}}^{(5)}(M_Z^2)$ -shift, remains below or of the order of the present error value on $\Delta\alpha_{\text{had}}^{(5)}(M_Z^2)$ (the thick green line).

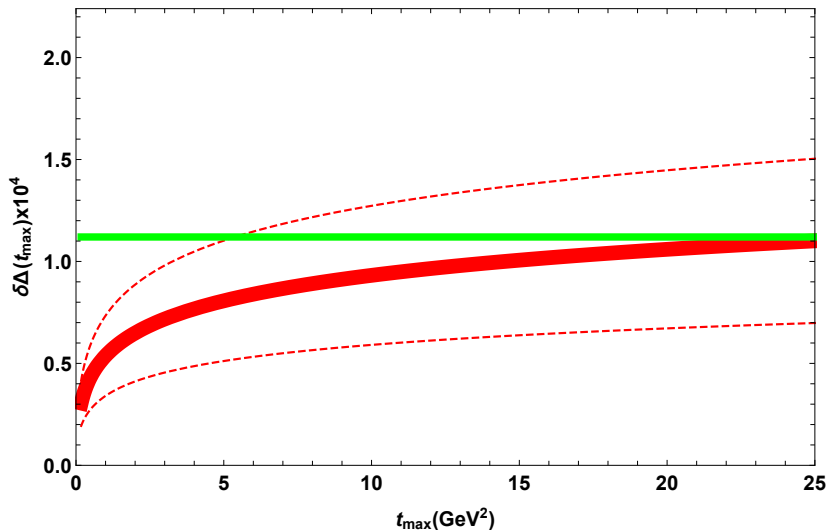


Figure 2:

Size of the $\delta\Delta\alpha_{\text{had}}^{(5)}(M_Z^2)$ -shift in 10^{-4} units as a function of the t_{\max} -choice. The thick red curve shows the shift corresponding to the central value of the discrepancy Δa_μ ; the dashed curves the same shift when including the upper and lower errors on Δa_μ . The thick green line shows the present experimental error on $\Delta\alpha_{\text{had}}^{(5)}(M_Z^2)$, also in 10^{-4} units.

VI Summary and Conclusions.

- The bounds in Eq. (4.12) are rigorous minimal bounds on the $\delta\Delta\alpha_{\text{had}}^{(5)}(M_Z^2)$ -shift implied by the Δa_μ -discrepancy in Eq. (1.11). They do not assume any specific shape of energy dependence

in the underlying spectral function $\frac{1}{\pi}\text{Im}\Delta(t)$ which is at the origin of the discrepancy. In the absence of any information about the shape of $\frac{1}{\pi}\text{Im}\Delta(t)$ this is as much as can be said at present.

- The simple Quark Model discussed above illustrates the fact that it is possible to construct spectral functions which reproduce the two anomaly values $a_\mu(\text{BMWc})$ and $a_\mu(\text{KNT})$ and yet, their difference, induces a shift on $\Delta\alpha_{\text{had}}^{(5)}(M_Z^2)$ which although larger than the upper minimal bound in Eq. (4.12), is still much smaller than the present error in Eq. (1.9).
- Finally, I have discussed the scenario where the underlying spectral function $\frac{1}{\pi}\text{Im}\Delta(t)$ responsible for the Δa_μ -discrepancy could be constant in a finite t -range: from threshold $t_{\text{min}} = 4m_\pi^2$ up to an arbitrary $t_{\text{max}} \ll M_Z^2$ and show that in this case the Δa_μ -discrepancy induces a $\delta\Delta\alpha_{\text{had}}^{(5)}(M_Z^2)$ -shift which, as shown in Fig. (2), remains compatible with the present data-driven determination of $\Delta\alpha_{\text{had}}^{(5)}(M_Z^2)$ up to $t_{\text{max}} \lesssim 5 \text{ GeV}^2$ -values.

Acknowledgements

I am very much indebted to my colleagues: Laurent Lellouch, Marc Knecht, David Greynat and Jérôme Charles, for their generous help and their suggestions to improve the contents of this note. Discussions with the authors of ref. [13] are also acknowledged. I also wish to thank the referee for suggesting improvements and clarifications.

References

- [1] M. Steinhauser, Phys. Lett. **B429** 158 (1998).
- [2] C. Sturm, Nucl. Phys. **B874** 698 (2013).
- [3] C. Bouchiat and L. Michel, J. Phys. Radium **22** 121 (1961).
- [4] M. Gourdin and E. de Rafael, Nucl. Phys. **B10** 667 (1969).
- [5] B.E. Lautrup, A. Peterman and E. de Rafael, Phys. Rep. **C3** 193 (1972).
- [6] E. de Rafael, Phys. Lett. **B322** 239 (1994).
- [7] T. Blum, Phys. Rev. Lett. **91** 052001 (2003).
- [8] M. Davier, A. Hoecker, B. Malaescu, and Z. Zhang, Eur. Phys. J. **C80**, 241 (2020).
- [9] A. Keshavarzi, D. Nomura, and T. Teubner, Phys. Rev. **D101**, 014029 (2020).
- [10] T. Aoyama *et al*, **White Paper**: The anomalous magnetic moment of the muon in the Standard Model, arXiv:2006.04822v1 [hep-ph] 8 Jun 2020.
- [11] Sz. Borsanyi *et al* (BMWc-collaboration), arXiv:2002.12347v2 [hep-lat] 18 Aug 2020.
- [12] M. Passera, W.J. Marciano and A. Sirlin, Phys. Rev. **D78**, 013009 (2008).
- [13] A. Crivellin, M. Hoferichter, C.A. Manzari and M. Montull, arXiv:2003.04886v2 [hep-ph] 7 May 2020.
- [14] A. Keshavarzi, W.J. Marciano, M. Passera and A. Sirlin, arXiv:2006.12666v2 [hep-ph] 24 August 2020.
- [15] B. Malaescu and M. Scott, arXiv:2008.08107v1 [hep-ph] 18 Aug 2020.

- [16] E. de Rafael, Phys. Letters **B736** 52 (2014).
- [17] E. de Rafael, Phys. Rev. **D96** 014510 (2017).
- [18] J. Charles, D. Greynat and E. de Rafael, Phys. Rev. **D97** 076014 (2018).
- [19] D. Greynat, *unpublished*.
- [20] E. Braaten, S. Narison and A. Pich, Nucl. Phys. **B373** 581 (1992).
- [21] J.S. Bell and E. de Rafael, Nucl. Phys. **B11** 611 (1969).
- [22] D. Greynat and E. de Rafael, JHEP **07** 020 (2012).